



Ultrafast ultrasound coupled with cervical magnetic stimulation for non-invasive and non-volitional assessment of diaphragm contractility

Thomas Poulard, Martin Dres, Marie-Cécile Nierat, Isabelle Rivals, Jean-Yves Hogrel, Thomas Similowski, Jean-Luc Gennisson, Damien Bachasson

► To cite this version:

Thomas Poulard, Martin Dres, Marie-Cécile Nierat, Isabelle Rivals, Jean-Yves Hogrel, et al.. Ultrafast ultrasound coupled with cervical magnetic stimulation for non-invasive and non-volitional assessment of diaphragm contractility. *The Journal of Physiology*, 2020, 598 (24), pp.5627-5638. 10.1113/JP280457 . hal-03266752

HAL Id: hal-03266752

<https://hal.sorbonne-universite.fr/hal-03266752>

Submitted on 22 Jun 2021

HAL is a multi-disciplinary open access archive for the deposit and dissemination of scientific research documents, whether they are published or not. The documents may come from teaching and research institutions in France or abroad, or from public or private research centers.

L'archive ouverte pluridisciplinaire **HAL**, est destinée au dépôt et à la diffusion de documents scientifiques de niveau recherche, publiés ou non, émanant des établissements d'enseignement et de recherche français ou étrangers, des laboratoires publics ou privés.

The Journal of Physiology

<https://jp.msubmit.net>

JP-TFP-2020-280457R2

Title: Ultrafast ultrasound coupled with cervical magnetic stimulation for non-invasive and non-volitional assessment of diaphragm contractility

Authors: Thomas Poulard
Martin Dres
Marie-Cécile Nierat
Isabelle Rivals
Jean-Yves Hogrel
Thomas Similowski
Jean-Luc Gennisson
Damien Bachasson

Author Conflict: Martin Dres: MD received personal fees from Lungpacer. Jean-Luc Gennisson: JLG is a scientific consultant for Supersonic Imagine, Aix-en-Provence, France.

Author Contribution: Thomas Poulard: Conception or design of the work; Acquisition or analysis or interpretation of data for the work; Drafting the work or revising it critically for important intellectual content; Final approval of the version to be published; Agreement to be accountable for all aspects of the work Martin Dres: Conception or design of the work; Drafting the work or revising it critically for important intellectual content; Final approval of the version to be published; Agreement to be accountable for all aspects of the work Marie-Cécile Nierat: Conception or design of the work; Drafting the work or revising it critically for important intellectual content; Final approval of the version to be published; Agreement to be accountable for all aspects of the work

Disclaimer: This is a confidential document.

Isabelle Rivals: Acquisition or analysis or interpretation of data for the work; Drafting the work or revising it critically for important intellectual content; Final approval of the version to be published; Agreement to be accountable for all aspects of the work Jean-Yves Hogrel: Conception or design of the work; Drafting the work or revising it critically for important intellectual content; Final approval of the version to be published; Agreement to be accountable for all aspects of the work Thomas Similowski: Conception or design of the work; Drafting the work or revising it critically for important intellectual content; Final approval of the version to be published; Agreement to be accountable for all aspects of the work Jean-Luc Gennisson: Conception or design of the work; Acquisition or analysis or interpretation of data for the work; Drafting the work or revising it critically for important intellectual content; Final approval of the version to be published; Agreement to be accountable for all aspects of the work Damien Bachasson: Conception or design of the work; Acquisition or analysis or interpretation of data for the work; Drafting the work or revising it critically for important intellectual content; Final approval of the version to be published; Agreement to be accountable for all aspects of the work

Running Title: Ultrafast ultrasound imaging of the diaphragm

Dual Publication: No

Funding: Fondation EDF: Thomas Poulard, Jean-Yves Hogrel, Damien Bachasson, N/A; Association Francaise contre les Myopathies (Association Française contre les Myopathies): Thomas Poulard, Jean-Yves Hogrel, Damien Bachasson, N/A The PhD fellowship of TP is funded by the Fondation EDF that is supporting the RespiMyo project, which includes the current study. This study was also supported by the Association Française Contre Les Myopathies (AFM).

1 **Ultrafast ultrasound coupled with cervical magnetic**
2 **stimulation for non-invasive and non-volitional**
3 **assessment of diaphragm contractility**

4 Thomas Poulard^{1,2}, Martin Dres^{3,4}, Marie-Cécile Niérat³, Isabelle Rivals⁵, Jean-Yves
5 Hogrel², Thomas Similowski^{3,4}, Jean-Luc Gennisson^{1#}, Damien Bachasson^{2##*}

6 *#equally contributing authors*

7

8

9 ¹ Laboratoire d'Imagerie Biomédicale Multimodale, BioMaps, Université Paris-Saclay,
10 CEA, CNRS UMR 9011, Inserm UMR1281, SHFJ, 4 place du général Leclerc, 91401, Orsay,
11 France

12 ² Institute of Myology, Neuromuscular Investigation Center, Neuromuscular Physiology
13 Laboratory, Paris, France

14 ³ Sorbonne Université, INSERM, UMRS1158 Neurophysiologie respiratoire expérimentale
15 et clinique, Paris, France

16 ⁴ AP-HP. Sorbonne Université, Hôpital Pitié-Salpêtrière, Service de Pneumologie, Médecine
17 intensive – Réanimation (Département "R3S"), F-75013, Paris, France

18 ⁵ Equipe de Statistique Appliquée, ESPCI Paris, PSL Research University, UMRS 1158, 10
19 rue Vauquelin, 75005, Paris, France

20

21 *Corresponding author: Damien Bachasson, PhD. Institut de Myologie, Laboratoire de
22 Physiologie et d'Evaluation Neuromusculaire, Hôpital Universitaire Pitié Salpêtrière, Paris
23 75651 Cedex 13, France. Tel: +33 1 42 16 66 41; fax: +33 1 42 16 58 81. E-mail:
24 d.bachasson@institut-myologie.org

25 **Table of contents categories**

26 Respiratory

27

28 **Key points summary**

- 29 • Twitch transdiaphragmatic pressure elicited by cervical magnetic stimulation of the
30 phrenic nerves is a fully non-volitional method for assessing diaphragm contractility
31 in humans, yet it requires invasive procedures such as esophageal and gastric catheter-
32 balloons.
- 33 • Ultrafast ultrasound enables a very high frame rate allowing the capture of transient
34 events, such as muscle contraction elicited by nerve stimulation (twitch). Whether
35 indices derived from ultrafast ultrasound can be used as an alternative to the invasive
36 measurement of twitch transdiaphragmatic pressure is unknown.
- 37 • Our findings demonstrate that maximal diaphragm tissue velocity assessed using
38 ultrafast ultrasound following cervical magnetic stimulation is reliable, sensitive to
39 change in cervical magnetic stimulation intensity, and correlates to twitch
40 transdiaphragmatic pressure.
- 41 • This approach provides a novel fully non-invasive and non-volitional tool for the
42 assessment of diaphragm contractility in humans.

43 **Abstract**

44 Measuring twitch transdiaphragmatic pressure ($P_{di,tw}$) elicited by cervical magnetic
45 stimulation (CMS) is considered as a reference method for the standardized evaluation of
46 diaphragm function. Yet, the measurement of P_{di} requires invasive esophageal and gastric
47 catheter-balloons. Ultrafast ultrasound is a non-invasive imaging technique enabling frame
48 rates high enough to capture transient events such as evoked muscle contractions. This study
49 investigated relationships between indices derived from ultrafast ultrasounds and $P_{di,tw}$, and
50 how these indices may be used to estimate $P_{di,tw}$. CMS was performed in 13 healthy
51 volunteers from 30 to 100 % of stimulator intensity in units of 10 % in a randomized order.
52 $P_{di,tw}$ was measured and the right hemidiaphragm was imaged using a custom ultrafast
53 ultrasound sequence with 1 kHz framerate. Maximal diaphragm axial velocity ($V_{di,max}$) and
54 diaphragm thickening fraction ($TF_{di,tw}$) were computed. Intra-session reliability was
55 assessed. Repeated-measures correlation (R) and Spearman correlation coefficients (ρ) were
56 used to assess relationships between variables. Intra-session reliability was strong for $P_{di,tw}$
57 and $V_{di,max}$ and moderate for $TF_{di,tw}$. $V_{di,max}$ correlated with $P_{di,tw}$ in all subjects ($0.64 < \rho <$
58 1.00 , $R = 0.75$; all $p < 0.05$). $TF_{di,tw}$ correlated with $P_{di,tw}$ in 8 subjects only ($0.85 < \rho < 0.93$,
59 $R = 0.69$; all $p < 0.05$). Coupling ultrafast ultrasound and CMS show promise for the non-
60 invasive and fully non-volitional assessment of diaphragm contractility. This approach opens
61 up prospects for both diagnosis and follow-up of diaphragm contractility in clinical
62 populations.

63

64 **Key Words:** Diaphragm, ultrafast ultrasound imaging, cervical magnetic stimulation,
65 skeletal muscle, contractility, phrenic nerves

66 Introduction

67 Sixty years ago, [Agostoni & Rahn, \(1960\)](#) introduced a novel method to measure the
68 specific contribution of the diaphragm to the intrathoracic pressure generated during
69 inspiratory efforts, namely, transdiaphragmatic pressure (Pdi). Pdi is defined as the difference
70 between gastric (Pga) and esophageal (Pes) pressures measured using gastric and esophageal
71 probes. Twitch Pdi (Pdi_{tw}) elicited by cervical magnetic stimulation (CMS) was introduced
72 30 years ago and is considered as a reference method for the non-volitional assessment of
73 diaphragm contractility ([Similowski et al., 1989](#)). Yet, measuring Pdi_{tw} is considered invasive
74 and requires a high level of expertise ([Laveneziana et al., 2019](#)). Twitch mouth pressure
75 (Pmo_{tw}) or nasal mask twitch pressure have been developed as an alternative to Pdi_{tw} ([Yan et](#)
76 [al., 1992; Teixeira et al., 2007](#)). However, this approach requires some degree of cooperation
77 from the subjects because small inspiratory/expiratory efforts ([Similowski et al., 1993](#);
78 [Hamnegaard et al., 1995](#); [Windisch et al., 2005](#); [Kabitz et al., 2007](#)) are required prior the
79 stimulation to prevent upper airway collapse and/or glottis closure and ensure adequate
80 transmission. Moreover, these procedures required proper mouth occlusion, which cannot be
81 performed in many patients such as patients with neuromuscular disorders.

82 Ultrasound (US) imaging has emerged as a tool for assessing the diaphragm ([Ueki et](#)
83 [al., 1995](#)) and is increasingly used in clinical settings such as the intensive care unit ([Dres &](#)
84 [Demoule, 2020](#)). Imaging of the zone of apposition of the right-hemidiaphragm is classically
85 performed to investigate diaphragm behavior. Various indices can be derived from
86 diaphragm US such as diaphragm excursion or thickening fraction ([Goligher et al., 2015](#);
87 [Tuinman et al., 2020](#)), diaphragm strain ([Oppersma et al., 2017](#)), or more recently changes
88 in diaphragm stiffness assessed with US shear wave elastography ([Bachasson et al., 2019](#)).
89 However, these methods offer limited frame rate (i.e. a few tens of frames per second for
90 standard US and a few frames per second for US shear wave elastography). Therefore, these
91 methods cannot be used for capturing fast transient phenomena, such as diaphragm response
92 elicited by CMS (~300 ms).

93 Ultrafast US is a fairly recent imaging technique enabling very high frame rates (up
94 to 20 kHz, ([Sandrin et al., 1999](#))). This technique has previously been used in the biceps

95 brachii to visualize muscle behavior during short-lasting contractions ([Deffieux et al., 2008](#);
96 [Gronlund et al., 2013](#)). By performing a radio frequency-based speckle tracking, ultrafast US
97 allows the quantification of transient velocities of mechanical waves induced by
98 transcutaneous electrical stimulation ([Deffieux et al., 2008](#)). Maximal tissue velocity has
99 been reported to increase linearly with stimulation intensity. However, the relationship
100 between tissue velocity and the force generated by the muscle during stimulation is unknown.
101 In a recent pilot work, we reported that diaphragm response elicited by CMS can be imaged
102 using ultrafast US and that responses elicited at high and low stimulation intensity can be
103 discriminated ([Bachasson et al., 2018](#)). However, the relationship between diaphragm
104 pressure generation and indices derived from ultrafast US during CMS remains to be
105 thoroughly investigated.

106 Therefore, this study aimed at imaging the diaphragm during CMS at different
107 intensity levels using ultrafast US. By investigating the relationships between $P_{di,tw}$ and
108 indices derived from ultrafast US imaging (i.e. thickening fraction, maximal tissue velocity),
109 we hypothesized that diaphragm thickening fraction and diaphragm tissue velocity following
110 CMS were correlated to $P_{di,tw}$, and that these indices may be used as a surrogate to $P_{di,tw}$.

111 **Methods**

112 **Ethical approval**

113 This study conformed to the Declaration of Helsinki. It was approved by the local
114 ethics committee (Comité de Protection des Personnes Île-de-France VI, France, February
115 22nd 2016, ID-RCB 2015-A00949-40) and was publicly registered before the first inclusion
116 (ClinicalTrials.gov, NCT03313141). All participants gave written informed consent. Some
117 of the data from this study have already been published elsewhere, regarding the use of
118 diaphragm shear wave elastography in healthy subjects during ventilation ([Bachasson et al.,](#)
119 [2019](#)).

120 **Participants**

Ultrafast ultrasound imaging of the diaphragm

121 Thirteen healthy participants (5 males and 8 females, median (Q1-Q3) – age = 24 (22-
122 27) years, height = 171 (167-183) cm, BMI = 20.6 (19.7-22.6) kg.m⁻²) were studied.
123 Participants had to be 18 and over with no history of respiratory or neuromuscular disorders,
124 and no contraindication to CMS ([Rossi et al., 2011](#)).

125 Pressure measurements

126 Participants were studied in a semirecumbent position (~45 degrees) with uncast
127 abdomen. Pes and Pga were measured using 8 cm balloon catheters (Marquat Genie
128 Biomedical, Boissy-Saint-Léger Cedex, France). Balloons were introduced through the
129 participant's nostril and both placed in the stomach so that a positive pressure deflection was
130 monitored when gently pressing the participant's stomach. Subsequently, one balloon was
131 slowly withdrawn toward the esophagus until the pressure deflection was no more monitored
132 when pressing the participant's stomach, and was then withdrawn an additional 10 cm.
133 Esophageal balloon position was adjusted using the Baydur maneuver ([Baydur et al., 1982](#)).
134 Balloons were then connected to differential pressure transducers (MLT0380/D,
135 ADInstruments, Bella Vista, Australia) and filled with 4 and 5.5 ml of air in the esophageal
136 and gastric balloons, respectively ([Mojoli et al., 2015](#)). All signals were digitized at a 4 kHz
137 frequency using a PowerLab system (16/35, ADInstruments, Bella Vista, Australia) and
138 recorded on the LabChart software. Pdi was computed as the difference between Pga and
139 Pes.

140 Cervical Magnetic Stimulation

141 CMS was performed using a Magstim 200 stimulator (Magstim, Whitland, Dyfed,
142 UK) driving a 90-mm circular coil (1 Tesla maximum output) as previously described
143 ([Similowski et al., 1989](#)). Briefly, participants were asked to bend their neck forward and the
144 central hole of the coil was positioned on the spinous process of the seventh cervical vertebra.
145 Optimal coil position was determined by performing a series of stimulation at 100 % of
146 stimulator intensity. The spot where Pdi_{tw} was the highest was skin-marked and kept constant
147 during the whole experiment.

148 Ultrafast ultrasound imaging

149 The zone of apposition of the right hemidiaphragm was imaged using a 6 MHz central
150 frequency linear transducer (SL 10-2) driven by an ultrafast ultrasound device (Aixplorer
151 V12, Supersonic Imagine, Aix-en-Provence, France). The probe was placed on the mid-
152 axillary line, vertical to the chest wall, at the 8th-10th intercostal space. The site of the probe
153 placement was skin-marked to ensure that the same region of interest was imaged during the
154 whole protocol. The diaphragm was identified as a three-layers structure superficial to the
155 liver, with two hyperechoic layers (*i.e.* the *pleura* and *peritoneum*) surrounding a hypoechoic
156 muscular layer (Figure 1). As the duration of P_{ditw} is ~ 300 ms, a custom ultrafast US
157 sequence was designed to track diaphragm movements during this time window. The
158 sequence was composed of 9 plane-wave US with different angles (-7° to 7° with a 2°
159 incremental steps) at 9 kHz frame rate, yielding a compounded frame rate of 1 kHz and a 500
160 ms ([Montaldo et al., 2009](#)). This sequence followed the Food and Drugs Administration
161 guidelines for acoustics norms (Mechanical index = 0.5, Thermal index = 0.2). Because
162 diaphragm depth rarely exceed 4 cm ([Shahgholi et al., 2014](#)), the US sequence was developed
163 in order to maintain the same spatial and temporal resolution of to this depth of 4 cm. Such
164 sequence allows the imaging of the diaphragm in overweight patients. Signals were
165 synchronized using an output trigger sent from the ultrafast US device to the Powerlab
166 system. A fixed delay of 100 ms was set between the onset of US recordings and CMS, after
167 which the stimulator was triggered by the Powerlab for delivering the stimulation. Recording
168 of pressure signals was started 1 s before the US trigger. The experimental setup and
169 procedure for recording pressure and US frames is displayed in Figure 2. Of note, we
170 investigated whether diaphragm excursion elicited by CMS may be imaged during subcostal
171 scanning during pilot works. We measured very small excursion values that were highly
172 variable between trials. This finding was expected as diaphragm response elicited by CMS
173 is not associated with substantial change in pulmonary volume. This may be mainly
174 explained by glottis closure. Consequently, the measurement of diaphragm excursion during
175 CMS was not further explored.

176 **Experimental protocol**

177 *Cervical magnetic stimulations.* Participants were stimulated on the predefined optimal
178 stimulation spot from 30 to 100 % of stimulator intensity in units of 10 %, in a randomized
179 order. All stimulations were delivered at functional residual capacity (FRC). Lung volume
180 prior stimulation, estimated through Pes, was checked to be consistent across all stimulations.
181 A minimum of three stimulations, separated by at least one minute, were performed at each
182 stimulation intensity. Two to three validated trials (i.e. as indicated by appropriate Pes before
183 CMS) per intensity were considered for further analysis.

184 *Maximal voluntary maneuvers.* Participants were asked to perform maximal inspiratory
185 effort at residual volume. Maximal Pdi (Pdi_{max}) was measured using a unidirectional valve
186 allowing expiration only. Participants were asked to empty their lungs before being strongly
187 encouraged to generate maximal inspiratory effort. Visual feedback of Pdi was provided
188 during the maneuver. Three to five trials were performed and maximal pressure measured
189 over a 1 s period was recorded as Pdi_{max} . Sniff nasal inspiratory pressure (SNIP) was
190 determined as follows. Participants were asked to make a short and maximal sniff at FRC.
191 As recommended ([American Thoracic Society/European Respiratory, 2002](#)), participants
192 performed 8-10 attempts with a ~30-s rest in-between sniffs until a plateau of peak pressure
193 values was reached.

194 **Data analysis**

195 All data were analyzed offline using standardized Matlab scripts (Mathworks, Natick,
196 MA, USA). Pes, Pga, and Pdi signals were low-pass filtered (30 Hz) using a second-order
197 Butterworth filter. Esophageal twitch pressure (Pes_{tw}), gastric twitch pressure (Pga_{tw}), and
198 Pdi_{tw} following stimulation were calculated as the difference between maximal (for Pdi and
199 Pga) or minimal (for Pes) pressure and pressure at the onset of CMS.

200 Vertical speckle tracking was performed by computing the axial (i.e. perpendicular
201 to the ultrasound probe) relative displacements within the diaphragm. This technique consists
202 in comparing consecutive images using one-dimensional cross-correlations to measure the
203 relative displacement of a pixel between two consecutive frames ([Loupas et al., 1995](#)).
204 Diaphragm tissue velocity profile is then computed by dividing the measured displacement
205 by the time difference between two frames (i.e. 1 ms). As an example, Figure 3 shows how

206 the velocity within the diaphragm evolves over time. Diaphragm velocity was computed over
 207 each column of pixels within the diaphragm. The central third of each image was then
 208 averaged to obtain a single value of diaphragm velocity over time. This value was assumed
 209 to be representative of the whole diaphragm. Maximal diaphragm velocity ($V_{di\max}$) was then
 210 determined as the maximal (i.e. positive) velocity within this signal.

211 For each trial, a time-motion image was generated using the central pixel line of each
 212 ultrasound image, referred to as M-Mode in the following. The position of the *pleura* and
 213 *peritoneum* layers was then drawn manually over the full length of the M-Mode image. By
 214 doing so, diaphragm thickness (i.e. the difference between the *peritoneum* and *pleura*
 215 positions) was computed at each time of the US acquisition. Maximal diaphragm thickening
 216 fraction ($TF_{di\text{tw}}$) was computed using resting diaphragm thickness prior stimulation ($T_{di\text{rest}}$)
 217 and maximal diaphragm thickness following stimulation ($T_{di\max}$) as follows:

$$218 \quad TF_{di\text{tw}} (\%) = \frac{T_{di\max} - T_{di\text{rest}}}{T_{di\text{rest}}} \times 100 \quad [1]$$

219 All $TF_{di\text{tw}}$ measurements were performed by a single trained operator (TP), blinded to the
 220 stimulation intensity. A movie clip showing pressure signals, M-mode images, and indices
 221 derived from ultrafast US is available in supplementary materials S1.

222 Statistics

223 Results are presented as median (Q1-Q3) unless otherwise stated. Normality was assessed by
 224 visual inspection (*QQ plots* and density distributions) and by significance tests (*Shapiro-Wilk*
 225 *test*). Because all variables failed the normality test, Friedman repeated measures ANOVAs
 226 were used. ANOVAs were conducted to compare Pes prior to each stimulation at all
 227 stimulation intensities. Within-day reliability of $P_{di\text{tw}}$, $V_{di\max}$, and $TF_{di\text{tw}}$ was investigated.
 228 Standard errors of measurement (SEM) and intraclass correlation coefficients (ICC) were
 229 used to study absolute and relative reliability, respectively ([Hopkins, 2002](#)). The overall
 230 relationship between variables (R) was determined using repeated measure correlation
 231 ([Bakdash & Marusich, 2017](#)). This technique considers the independence of repeated
 232 measures between individuals, so that potential confounding factors, such as between-
 233 participant variability, do not interfere. Data are presented as R [95 % CI]. Spearman

correlation coefficients (ρ) were calculated to investigate within-individual relationships between variables. ANOVAs were used to assess the effect of stimulation intensity on Pdi_{tw} , Vdi_{max} , and $TFdi_{tw}$. Tukey's *post-hoc* tests were conducted if a significant main effect of intensity was found. Within individuals, Pdi_{tw} , Vdi_{max} , and $TFdi_{tw}$ were considered supramaximal if the average Pdi_{tw} , Vdi_{max} or $TFdi_{tw}$ at submaximal and maximal stimulation intensities was inferior or equal to the coefficient of variation of the variable at each stimulation intensities ([Welch et al., 2018](#); [Geary et al., 2019](#)). Supramaximality was reached if greater stimulation intensity did not result in further increase in Pdi_{tw} , Vdi_{max} or $TFdi_{tw}$. Analyses were performed in the computing environment R ([R Core Team, 2020](#)). Significance was set at $p<0.05$ for all tests.

Results

All participants completed the protocol. Pdi_{max} was 113 (71-115) cmH₂O 90 (56-117) cmH₂O in men and women, respectively. Overall, Pdi_{max} was 108 (71-117) cmH₂O. SNIP was 116 (109-130) cmH₂O in men and 103 (90-118) cmH₂O in women. Overall, SNIP was 109 (96-123) cmH₂O. The one-way repeated measures ANOVA showed that Pes at the onset of CMS was similar across all stimulations at all intensities ($p=0.2430$). Within-day SEM and ICC of Pdi_{tw} , Vdi_{max} , and $TFdi_{tw}$ are presented in Table 1. Typical B-Mode images over the course of the 500 ms US acquisition are presented in supplementary materials S2.

Effect of stimulation intensity on indices derived from ultrafast ultrasound

M-Mode images and temporal evolution of the displacements of the *pleura* and *peritoneum*, Vdi_{max} , and recorded pressures in one individual are displayed in Figure 4 (also see movie clip in Supporting Information S1). Pes_{tw} , Pga_{tw} , and Pdi_{tw} at all tested stimulation intensities are shown in Figure 5 and Figure 6A. Vdi_{max} and $TFdi_{tw}$ at all tested stimulation intensities are displayed in Figure 6B-C. Within individual relationships between stimulation intensity and Pdi_{tw} , Vdi_{max} , and $TFdi_{tw}$ are shown in Figure 6D-F.

Pdi_{tw} was significantly related to stimulation intensity in all subjects (ρ ranged from 0.83 to 1.00, all $p<0.0100$; $R = 0.91$, 95 % CIs [0.86 0.94], $p<0.0001$). At the group level, there was a significant main effect of stimulation intensity on Pdi_{tw} . *Post-hoc* tests indicated

Ultrafast ultrasound imaging of the diaphragm

262 that Pdi_{tw} significantly increased up to 100 % of stimulation intensity (all $p<0.05$). Within
263 individuals, Pdi_{tw} plateaued at 90 % of stimulation intensity in two participants. In other
264 participants, Pdi_{tw} increased until 100 % of stimulation intensity.

265 Vdi_{max} correlated to stimulation intensity in all participants (ρ ranged from 0.79 to
266 1.00, all $p<0.0500$; $R = 0.83$, 95 % CIs [0.75 0.89], $p<0.0001$). At the group level, there was
267 a significant main effect of stimulation intensity on Vdi_{max} . *Post-hoc* tests indicated that
268 Vdi_{max} did not significantly differ between 90 and 100 % of stimulation intensity ($p=0.9997$).
269 No significant differences in Vdi_{max} was found between consecutive stimulation intensities,
270 except between 80 and 90 % of stimulation intensity ($p=0.0080$). Within individuals, Vdi_{max}
271 plateaued at 90 % of stimulation intensity in 6 participants, at 80 % in one participant, and at
272 70 % in one participant.

273 $TFdi_{tw}$ correlated to stimulation intensity ($R = 0.72$, 95 % CIs [0.60 0.80], $p<0.0001$).
274 Individual correlations were significant in 10 out of 13 subjects (ρ ranged from 0.67 to 0.95,
275 all $p<0.05$; ρ ranged from 0.33 to 0.52 in the three remaining participants, all $p>0.2200$). At
276 the group level, there was a significant main effect of stimulation intensity on $TFdi_{tw}$. *Post-*
277 *hoc* tests showed that $TFdi_{tw}$ did not significantly differ between 60 to 100% of stimulation
278 intensity (all $p>0.1155$). No significant differences in $TFdi_{tw}$ was found between consecutive
279 stimulation intensities. Within individuals, $TFdi_{tw}$ plateaued at 90 % of stimulation intensity
280 in 5 participants, at 80 % in two participants, at 70 % in two participants, at 50 % in one
281 participant and at 30 % in one participant. $TFdi_{tw}$ and Vdi_{max} at all stimulation intensities are
282 shown in Figure 6B and 6C, respectively.

283 Relationships between Pdi_{tw} and indices derived from ultrafast ultrasound

284 Within-individuals' relationships between Pdi_{tw} and Vdi_{max} , and between Pdi_{tw} and
285 $TFdi_{tw}$ are presented in Figure 7. Vdi_{max} correlated to Pdi_{tw} in all participants (ρ ranged from
286 0.64 to 1.00, all $p<0.05$; $R = 0.75$, 95 % CIs [0.65 0.83], $p<0.0001$). $TFdi_{tw}$ positively
287 correlated to Pdi_{tw} ($R = 0.69$, 95 % CIs [0.57 0.79], $p<0.0001$) and individual correlation
288 coefficients were significant in 8 out of 13 participants (ρ ranged from 0.85 to 0.93, all
289 $p<0.05$; ρ ranged from -0.27 to 0.70, in the five remaining participants, all $p>0.06$).

290 **Discussion**

291 This study is the first to image the diaphragm contraction induced by CMS using
292 ultrafast US. The main results are as follow: i) maximal tissue velocity within the diaphragm
293 significantly increased with stimulation intensity while diaphragm thickening fraction
294 plateaued at low stimulation intensity, ii) intra-session reliability of maximal tissue velocity
295 within the diaphragm was high and intra-session reliability of diaphragm thickening fraction
296 was poor iii) twitch transdiaphragmatic pressure strongly correlated with maximal tissue
297 velocity within the diaphragm and moderately correlated with diaphragm thickening fraction.

298 **Vdi_{max} is sensitive to changes in stimulation intensity and correlates to twitch
299 transdiaphragmatic pressure**

300 We found that Vdi_{max} increased with stimulation intensity in all participants. These
301 results are in line with previous works that reported a gradual increase in tissue velocity with
302 stimulation intensity during contractions elicited in the *biceps brachii* ([Deffieux et al., 2008](#);
303 [Gronlund et al., 2013](#)). To the best of our knowledge, this study is the first to report the
304 relationship between a muscle's tissue velocity and the force/pressure it produces. We found
305 that Vdi_{max} correlated to Pdi_{tw} in all participants, supporting that the magnitude of Vdi_{max} is
306 associated with the diaphragm contractility. Interestingly, Pdi_{tw} was supramaximal in two
307 subjects only, whereas Vdi_{max} was supramaximal in 8 subjects. The inability to reach
308 supramaximal Pdi_{tw} values in some subjects has been addressed before ([Man et al., 2004](#);
309 [Spiesshoefer et al., 2019](#)). This may be partly explained by insufficient magnetic stimulation
310 power to fully activate the phrenic nerves. It cannot be ruled out that supramaximality of
311 Pdi_{tw} occurred between 90 and 100 % of stimulation intensity. Nonetheless, it is known that
312 CMS at highest stimulation intensities stimulates neck muscles ([Attali et al., 1997](#)). Thus,
313 Pdi_{tw} is likely to increase not because of a higher activation of the diaphragm, but because
314 the recruitment of neck muscles increases the deflation of twitch Pes ([Wragg et al., 1994](#);
315 [Laghi et al., 1996](#)). Regarding Vdi_{max}, supramaximality was reached in 8 out of 13
316 participants. The fact that Vdi_{max} plateaued while Pdi_{tw} continued to increase may be related
317 to specificity of Vdi_{max} measurement, which directly probe the diaphragm. Therefore, Vdi_{max}
318 may be considered as a specific index of diaphragm contractility following CMS, ruling out

the confounding effects related to the recruitment of extra diaphragmatic muscle. Vdi_{max} did not meet supramaximality criteria in 5 subjects. Interestingly, 4 out of these 5 subjects did not reach supramaximality for Pdi_{tw} either. It can thus be suggested that the absence of Vdi_{max} supramaximality is directly related to the absence of Pdi_{tw} supramaximality. Also, one may observe that Vdi increases in the milliseconds following stimulation, while Pdi peaks ~ 150 ms after stimulation (Figure 4). This supports that the rapid change in Vdi correspond to diaphragm contraction and that this lag reflects the time needed for the diaphragm to transfer its force generation into an actual pressure generation. Importantly, Vdi_{max} was found to be strongly reproducible, as indicated by low SEM and high ICC that were comparable to those observed for Pdi_{tw} (Table 1). This high reliability build confidence regarding the potential of Vdi_{max} for non-volitional monitoring of diaphragm contractility over time. This study is also the first to report $TFdi_{tw}$ values during CMS. Repeated measure correlations showed a significant correlation between $TFdi_{tw}$ and stimulation intensity. Within individuals, 10 (77 %) participants presented with a significant relationship between $TFdi_{tw}$ and stimulation intensity. As compared to Vdi_{max} , $TFdi_{tw}$ was shown to be less sensitive to changes in stimulation intensity. At the group level, $TFdi_{tw}$ was moderately correlated to Pdi_{tw} . Our results are in line with previous studies that reported significant relationship between diaphragm thickening fraction and changes in Pdi during spontaneous breathing, inspiratory efforts, or in mechanically ventilated patients ([Ueki et al., 1995](#); [Vivier et al., 2012](#); [Goligher et al., 2015](#); [Umbrello et al., 2015](#)). However, when looking at individual relationship, the correlation between $TFdi_{tw}$ and Pdi_{tw} reached significance in 8 subjects (62%) only. We also found that $TFdi_{tw}$ plateaued at low stimulation intensity (60%). Importantly, the intra-session reliability of $TFdi_{tw}$ was rather poor. There are several potential explanations for these findings. First, $TFdi_{tw}$ was computed manually by drawing the position of the *pleura* and *peritoneum*. Imprecisions during this manual step might also be amplified by the lower image quality found using ultrafast US as compared to that of conventional US imaging. More specifically, conventional US imaging uses focused pulses, allowing for high image quality but a relatively low sampling rate (a few tens per second). On the other hand, ultrafast US plane wave imaging allows very high sampling rate (here, 1 kHz) but image quality is lower ([Montaldo et al., 2009](#)). Indeed, ultrafast US prevents the focusing of US beams to a specific

349 tissue (i.e. in this case, the diaphragm) and negatively impacts the signal to noise ratio of the
350 resulting image. As a result, the ultrafast US sequence developed for the current experiment
351 does not allow strong contrast of anatomic structures in comparison to standard US imaging
352 (Figure 1A). This may disrupt the measurement of TFdi_{tw} (Figure 1B) and contribute to
353 explain the low intra-session reliability of TFdi_{tw} indicated by the substantial SEM (~10%)
354 and moderate ICC (<0.6). Noteworthy, TFdi during ventilation was previously shown to be
355 moderately reliable using traditional ultrasound imaging ([Goligher et al., 2015](#)). This low
356 reliability may explain, at least in part, the absence of increase in TFdi_{tw} with increasing
357 stimulation intensity and increasing Pdi_{tw} in some participants. Indeed, we found in some
358 participants that TFdi_{tw} plateaued at intensities as low as 40—60 %. Because of the large
359 increase in Pdi_{tw} between 60 and 100 % of stimulation intensity, it is very unlikely that
360 supramaximal TFdi_{tw} values depicts full diaphragm recruitment. All together, these findings
361 suggest that TFdi_{tw} may be of limited help to assess diaphragm contractility in response to
362 CMS.

363 **Perspectives and limitations**

364 We demonstrated that Vdi_{max} was strongly related to Pdi_{tw} in all subjects. This could
365 have important implications for monitoring temporal changes in diaphragm contractility in
366 patients presenting with diaphragm dysfunction. In other words, Vdi_{max} elicited by CMS
367 could be monitored over time using ultrafast US, allowing iterative, specific, fully non-
368 invasive and non-volitional assessment of diaphragm contractility. It is worth noting that
369 between-subject variability was relatively important. In turn, one may question how Vdi_{max}
370 may be used to identify diaphragm dysfunction. Further studies will focus on this specific
371 point, with the perspective that Vdi_{max} may be one parameter, among others, guiding
372 clinicians through the assessment of diaphragm contractility. Inter-operator and between day
373 reliability of Vdi_{max} remains to be investigated. Assessing the delay between CMS and
374 diaphragm response as assessed using Vdi_{max} may also be promising to investigate both
375 phrenic conduction and electromechanical delay. Unfortunately, EMG was not available in
376 the current study and this shall be investigated in future works. As mentioned above, we
377 cannot ensure that supramaximality was achieved in all subjects. It is possible that

Ultrafast ultrasound imaging of the diaphragm

maximality occurred between 90 and 100 % of stimulation intensity in some subjects. This problem has been addressed before ([Man et al., 2004](#); [Spiesshoefer et al., 2019](#)), but can be considered negligible if a rigorous and standardized study-design is routinely used. Also, as the primary aim of this study was to detect changes in diaphragm contractility according to stimulation intensity and relationships between variables, supramaximality should not be considered as an important concern. We also emphasize that only the right hemidiaphragm was imaged in this study and that future works shall thoroughly investigate this approach in the left hemidiaphragm. Lastly, the ultrafast US sequence used in this study was custom-made so that the present approach cannot be readily generalized to clinical environments as it required a specific US scanner, US sequences that are not available commercially, specific training, and represent a non-negligible costs.

Conclusion

These study shows that ultrafast US may be used to image diaphragm behavior following CMS. Diaphragm tissue velocity is strongly correlated with twitch transdiaphragmatic pressure and appears to be highly specific to diaphragm contractility. Further research is warranted to investigate how ultrafast US may be used in patients, in particular those with diaphragm dysfunction. Coupling ultrafast US with CMS opens prospect for a fully non-invasive, non-volitional assessment and follow-up of diaphragm contractility in clinical populations.

397 **Additional information**

398 **Data Availability Statement**

399 The data that support the findings of this study are available from the corresponding
400 author upon reasonable request.

401 **Competing interests**

402 JLG is a scientific consultant for Supersonic Imagine, Aix-en-Provence, France. MD
403 received personal fees from Lungpacer.

404 **Fundings**

405 The PhD fellowship of TP is funded by the *Fondation EDF* that is supporting the
406 RespiMyo project, which includes the current study. This study was also supported by the
407 *Association Française Contre Les Myopathies* (AFM).

408 **Author contributions**

409 All authors participated in the conception and design of the study. TP and DB
410 performed experiments. TP, JLG and DB analyzed the data and drafted the original version
411 of the manuscript. All authors critically revised and approved the final version of the
412 manuscript. All persons designated as authors qualify for authorship, and all those who
413 qualify for authorship are listed.

414 **Supporting information**

415 S1. A movie clip, slowed down 40 times, showing pressure signals, M-mode images,
416 and indices derived from ultrafast US is available at the following link:
417 <https://figshare.com/s/fe55c9aa033cb6a42617>.

418 S2. A movie clip, in real-time, showing B-Mode and M-Mode images during a typical
419 500-ms ultrafast ultrasound acquisition is available at the following link:
420 <https://figshare.com/s/79fb82dd0361075df33e>

421 **References**

422

423 Agostoni E & Rahn H. (1960). Abdominal and thoracic pressures at different lung volumes.
424 *J Appl Physiol* **15**, 1087-1092.

425

426 American Thoracic Society/European Respiratory S. (2002). ATS/ERS Statement on
427 respiratory muscle testing. *Am J Respir Crit Care Med* **166**, 518-624.

428

429 Attali V, Mehiri S, Straus C, Salachas F, Arnulf I, Meininger V, Derenne JP & Similowski
430 T. (1997). Influence of neck muscles on mouth pressure response to cervical magnetic
431 stimulation. *Am J Respir Crit Care Med* **156**, 509-514.

432

433 Bachasson D, Dres M, Nierat M, Doorduin J, Gennisson J, Hogrel J & Similowski T. (2018).
434 Ultrafast Ultrasound Imaging Grants Alternate Methods for Assessing Diaphragm
435 Function. In *2018 IEEE International Ultrasonics Symposium (IUS)*, pp. 1-4.

436

437 Bachasson D, Dres M, Nierat MC, Gennisson JL, Hogrel JY, Doorduin J & Similowski T.
438 (2019). Diaphragm shear modulus reflects transdiaphragmatic pressure during
439 isovolumetric inspiratory efforts and ventilation against inspiratory loading. *J Appl
440 Physiol* (1985) **126**, 699-707.

441

442 Bakdash JZ & Marusich LR. (2017). Repeated Measures Correlation. *Front Psychol* **8**, 456.

443

444 Baydur A, Behrakis PK, Zin WA, Jaeger M & Milic-Emili J. (1982). A simple method for
445 assessing the validity of the esophageal balloon technique. *Am Rev Respir Dis* **126**,
446 788-791.

Ultrafast ultrasound imaging of the diaphragm

- 447
- 448 Deffieux T, Gennisson JL, Tanter M & Fink M. (2008). Assessment of the mechanical
449 properties of the musculoskeletal system using 2-D and 3-D very high frame rate
450 ultrasound. *IEEE Trans Ultrason Ferroelectr Freq Control* **55**, 2177-2190.
- 451
- 452 Dres M & Demoule A. (2020). Monitoring diaphragm function in the ICU. *Curr Opin Crit
453 Care* **26**, 18-25.
- 454
- 455 Geary CM, Welch JF, McDonald MR, Peters CM, Leahy MG, Reinhard PA & Sheel AW.
456 (2019). Diaphragm fatigue and inspiratory muscle metaboreflex in men and women
457 matched for absolute diaphragmatic work during pressure-threshold loading. *J
458 Physiol* **597**, 4797-4808.
- 459
- 460 Goligher EC, Laghi F, Detsky ME, Farias P, Murray A, Brace D, Brochard LJ, Bolz SS,
461 Rubenfeld GD, Kavanagh BP & Ferguson ND. (2015). Measuring diaphragm
462 thickness with ultrasound in mechanically ventilated patients: feasibility,
463 reproducibility and validity. *Intensive Care Med* **41**, 642-649.
- 464
- 465 Gronlund C, Claesson K & Holtermann A. (2013). Imaging two-dimensional mechanical
466 waves of skeletal muscle contraction. *Ultrasound Med Biol* **39**, 360-369.
- 467
- 468 Hamnegaard CH, Wragg S, Kyroussis D, Mills G, Bake B, Green M & Moxham J. (1995).
469 Mouth pressure in response to magnetic stimulation of the phrenic nerves. *Thorax* **50**,
470 620-624.
- 471
- 472 Hopkins W. (2002). A new view of statistics: Effect magnitudes. *Retrieved February 14,*
473 2005.

- 474
- 475 Kabitz HJ, Walker D, Walterspacher S & Windisch W. (2007). Controlled twitch mouth
476 pressure reliably predicts twitch esophageal pressure. *Respir Physiol Neurobiol* **156**,
477 276-282.
- 478
- 479 Laghi F, Harrison MJ & Tobin MJ. (1996). Comparison of magnetic and electrical phrenic
480 nerve stimulation in assessment of diaphragmatic contractility. *J Appl Physiol (1985)*
481 **80**, 1731-1742.
- 482
- 483 Laveneziana P, Albuquerque A, Aliverti A, Babb T, Barreiro E, Dres M, Dubé B-P, Fauroux
484 B, Gea J, Guenette JA, Hudson AL, Kabitz H-J, Laghi F, Langer D, Luo Y-M, Alberto
485 Neder J, O'Donnell D, Polkey MI, Rabinovich RA, Rossi A, Series F, Similowski T,
486 Spengler C, Vogiatzis I & Verges S. (2019). ERS Statement on Respiratory Muscle
487 Testing at Rest and during Exercise. *European Respiratory Journal*, 1801214.
- 488
- 489 Loupas T, Powers JT & Gill RW. (1995). An axial velocity estimator for ultrasound blood
490 flow imaging, based on a full evaluation of the Doppler equation by means of a two-
491 dimensional autocorrelation approach. *IEEE Transactions on Ultrasonics,
492 Ferroelectrics, and Frequency Control* **42**, 672-688.
- 493
- 494 Man WD, Moxham J & Polkey MI. (2004). Magnetic stimulation for the measurement of
495 respiratory and skeletal muscle function. *Eur Respir J* **24**, 846-860.
- 496
- 497 Mojoli F, Chiumello D, Pozzi M, Algieri I, Bianzina S, Luoni S, Volta CA, Braschi A &
498 Brochard L. (2015). Esophageal pressure measurements under different conditions of
499 intrathoracic pressure. An in vitro study of second generation balloon catheters.
500 *Minerva Anestesiol* **81**, 855-864.
- 501

Ultrafast ultrasound imaging of the diaphragm

- 502 Montaldo G, Tanter M, Bercoff J, Benech N & Fink M. (2009). Coherent plane-wave
503 compounding for very high frame rate ultrasonography and transient elastography.
504 *IEEE Trans Ultrason Ferroelectr Freq Control* **56**, 489-506.
- 505
- 506 Oppersma E, Hatam N, Doorduin J, van der Hoeven JG, Marx G, Goetzenich A, Fritsch S,
507 Heunks LMA & Bruells CS. (2017). Functional assessment of the diaphragm by
508 speckle tracking ultrasound during inspiratory loading. *J Appl Physiol (1985)* **123**,
509 1063-1070.
- 510
- 511 R Core Team. (2020). R: A Language and Environment for Statistical Computing. R
512 Foundation for Statistical Computing, Vienna, Austria.
- 513
- 514 Rossi S, Hallett M, Rossini PM & Pascual-Leone A. (2011). Screening questionnaire before
515 TMS: an update. *Clin Neurophysiol* **122**, 1686.
- 516
- 517 Sandrin L, Catheline S, Tanter M, Hennequin X & Fink M. (1999). Time-resolved pulsed
518 elastography with ultrafast ultrasonic imaging. *Ultrason Imaging* **21**, 259-272.
- 519
- 520 Shahgholi L, Baria MR, Sorenson EJ, Harper CJ, Watson JC, Strommen JA & Boon AJ.
521 (2014). Diaphragm depth in normal subjects. *Muscle Nerve* **49**, 666-668.
- 522
- 523 Similowski T, Fleury B, Launois S, Cathala HP, Bouche P & Derenne JP. (1989). Cervical
524 magnetic stimulation: a new painless method for bilateral phrenic nerve stimulation
525 in conscious humans. *J Appl Physiol (1985)* **67**, 1311-1318.
- 526

Ultrafast ultrasound imaging of the diaphragm

- 527 Similowski T, Gauthier AP, Yan S, Macklem PT & Bellemare F. (1993). Assessment of
528 diaphragm function using mouth pressure twitches in chronic obstructive pulmonary
529 disease patients. *Am Rev Respir Dis* **147**, 850-856.
- 530
- 531 Spiesshoefer J, Henke C, Herkenrath S, Brix T, Randerath W, Young P & Boentert M.
532 (2019). Transdiaphragmatic pressure and contractile properties of the diaphragm
533 following magnetic stimulation. *Respir Physiol Neurobiol* **266**, 47-53.
- 534
- 535 Teixeira A, Demoule A, Verin E, Morelot-Panzini C, Series F, Straus C & Similowski T.
536 (2007). Superiority of nasal mask pressure over mouth pressure, as a surrogate of
537 diaphragm twitch-related esophageal pressure, in healthy humans. *Respir Physiol
538 Neurobiol* **159**, 236-240.
- 539
- 540 Tuinman PR, Jonkman AH, Dres M, Shi ZH, Goligher EC, Goffi A, de Korte C, Demoule A
541 & Heunks L. (2020). Respiratory muscle ultrasonography: methodology, basic and
542 advanced principles and clinical applications in ICU and ED patients-a narrative
543 review. *Intensive Care Med* **46**, 594-605.
- 544
- 545 Ueki J, De Bruin PF & Pride NB. (1995). In vivo assessment of diaphragm contraction by
546 ultrasound in normal subjects. *Thorax* **50**, 1157-1161.
- 547
- 548 Umbrello M, Formenti P, Longhi D, Galimberti A, Piva I, Pezzi A, Mistraletti G, Marini JJ
549 & Iapichino G. (2015). Diaphragm ultrasound as indicator of respiratory effort in
550 critically ill patients undergoing assisted mechanical ventilation: a pilot clinical study.
551 *Crit Care* **19**, 161.
- 552

Ultrafast ultrasound imaging of the diaphragm

- 553 Vivier E, Mekontso Dessap A, Dimassi S, Vargas F, Lyazidi A, Thille AW & Brochard L.
554 (2012). Diaphragm ultrasonography to estimate the work of breathing during non-
555 invasive ventilation. *Intensive Care Med* **38**, 796-803.
- 556
- 557 Welch JF, Archiza B, Guenette JA, West CR & Sheel AW. (2018). Sex differences in
558 diaphragmatic fatigue: the cardiovascular response to inspiratory resistance. *J Physiol*
559 **596**, 4017-4032.
- 560
- 561 Windisch W, Kabitz HJ & Sorichter S. (2005). Influence of different trigger techniques on
562 twitch mouth pressure during bilateral anterior magnetic phrenic nerve stimulation.
563 *Chest* **128**, 190-195.
- 564
- 565 Wragg S, Aquilina R, Moran J, Ridding M, Hamnegard C, Fearn T, Green M & Moxham J.
566 (1994). Comparison of cervical magnetic stimulation and bilateral percutaneous
567 electrical stimulation of the phrenic nerves in normal subjects. *Eur Respir J* **7**, 1788-
568 1792.
- 569
- 570 Yan S, Gauthier AP, Similowski T, Macklem PT & Bellemare F. (1992). Evaluation of
571 human diaphragm contractility using mouth pressure twitches. *Am Rev Respir Dis*
572 **145**, 1064-1069.
- 573
- 574

575 **Tables**

576 **Table 1.** Within day reliability of twitch transdiaphragmatic pressure ($P_{di,tw}$), maximal
 577 diaphragm tissue velocity ($V_{di,max}$) and diaphragm thickening fraction ($TF_{di,tw}$) for all
 578 stimulations. SEM, standard error of measurement; ICC, intraclass correlation coefficient;
 579 [95% CI], 95% confidence interval.

580

Variable	Mean (SD)	SEM [95 % CI]	ICC [95 % CI]
$P_{di,tw}$ (cmH ₂ O)	11.6 (9.5)	1.55 [1.39 ; 1.75]	0.97 [0.96 ; 0.98]
$V_{di,max}$ (mm.s ⁻¹)	5.6 (5.0)	1.89 [1.70 ; 2.13]	0.86 [0.81 ; 0.90]
$TF_{di,tw}$ (%)	18.7 (15.6)	10.41 [9.38 ; 11.76]	0.56 [0.43 ; 0.66]

581

582

583 **Figures**

584 **Figure 1.** A. Typical B-Mode image of the diaphragm using conventional ultrasound
585 imaging. Conventional ultrasound uses focused pulses, allowing high image quality but
586 relatively low sampling rate (a few tens per second). The diaphragm can be identified as a
587 three-layers structure superficial to the liver. The echogenic *pleura* and *peritoneum* layers
588 surround the muscular layer of the diaphragm. B. The diaphragm is imaged using the custom
589 ultrafast ultrasound sequence used in this study. Noteworthy, ultrafast ultrasound allows very
590 high frame rate but limited contrast of anatomic structures in comparison to standard US
591 imaging.

592 **Figure 2.** Experimental setup and procedure for recording pressure and ultrafast ultrasound
593 images. The participants were asked to bend their neck forward and the central hole of the
594 coil was positioned on the spinous process of the seventh cervical vertebra. Recording of
595 pressure signals was initiated 1000 ms before the onset of ultrasound recording. Cervical
596 magnetic stimulation was applied 100 ms after the onset of a 500-ms ultrafast ultrasound
597 acquisition.

598 **Figure 3.** Diaphragm tissue velocity (V_{di}) over time along the longitudinal axis of the
599 ultrasound probe. Cervical magnetic stimulation occurs at 100 ms and is indicated by the
600 grey ribbon.

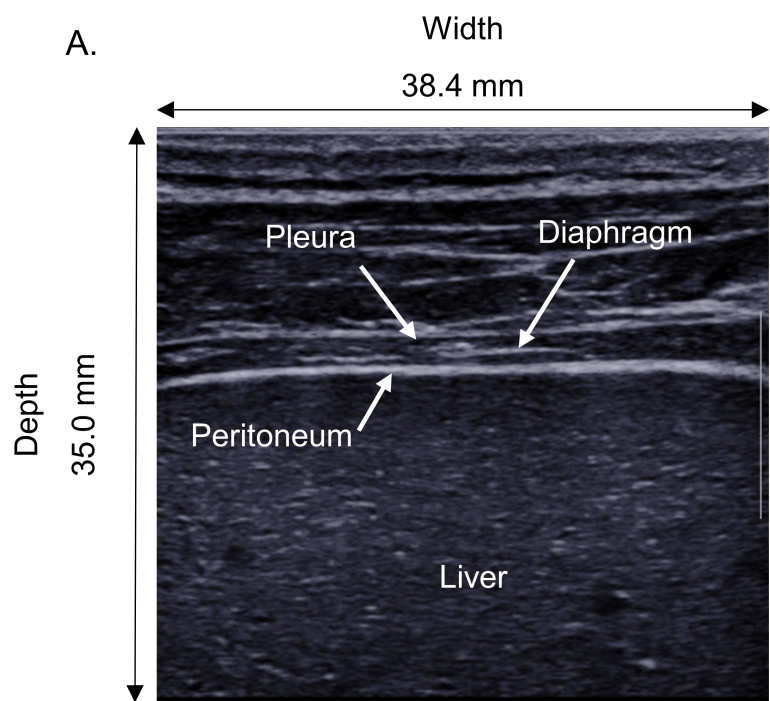
601 **Figure 4.** Typical ultrasound and physiological recordings at 40 (left), 70 (center) and 100
602 % (right) of stimulator intensity. The central pixel of each B-Mode image was used to
603 generate the M-Mode images (upper panel). *Pleura* (dashed) and *peritoneum* (solid) layers
604 displacement are presented in the second panel. Diaphragm tissue velocity (V_{di}) is presented
605 in the third panel. Lastly, the transdiaphragmatic (Pdi), esophageal (Pes) and gastric (Pga)
606 pressures are displayed in the bottom panel. The dotted vertical lines at 100 ms indicate the
607 onset of cervical magnetic stimulation.

608 **Figure 5.** Esophageal (P_{estw} , A.) and gastric (P_{gatw} , B.) twitch pressures at different
609 stimulation intensities. Box plots present first and third quartiles, in addition to the median.
610 The range over which the data spread out is defined by the whiskers.

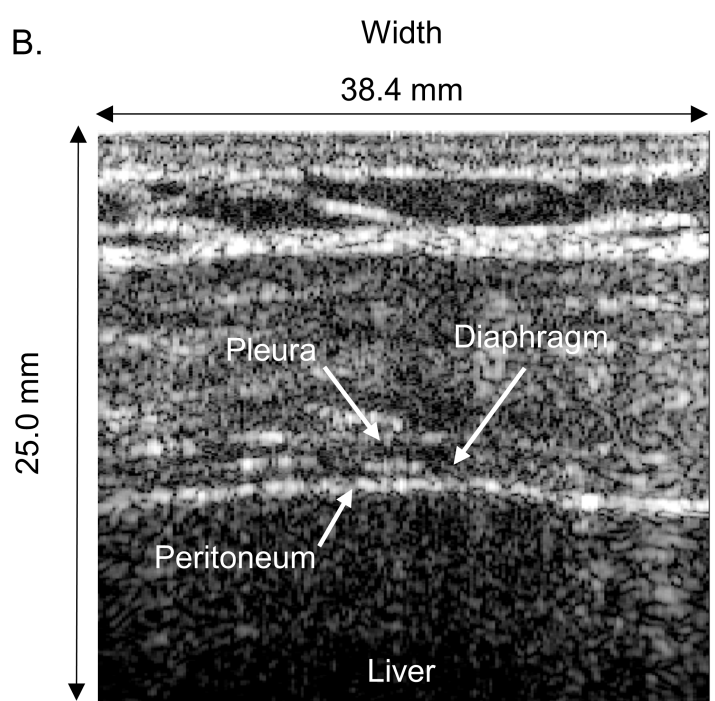
Ultrafast ultrasound imaging of the diaphragm

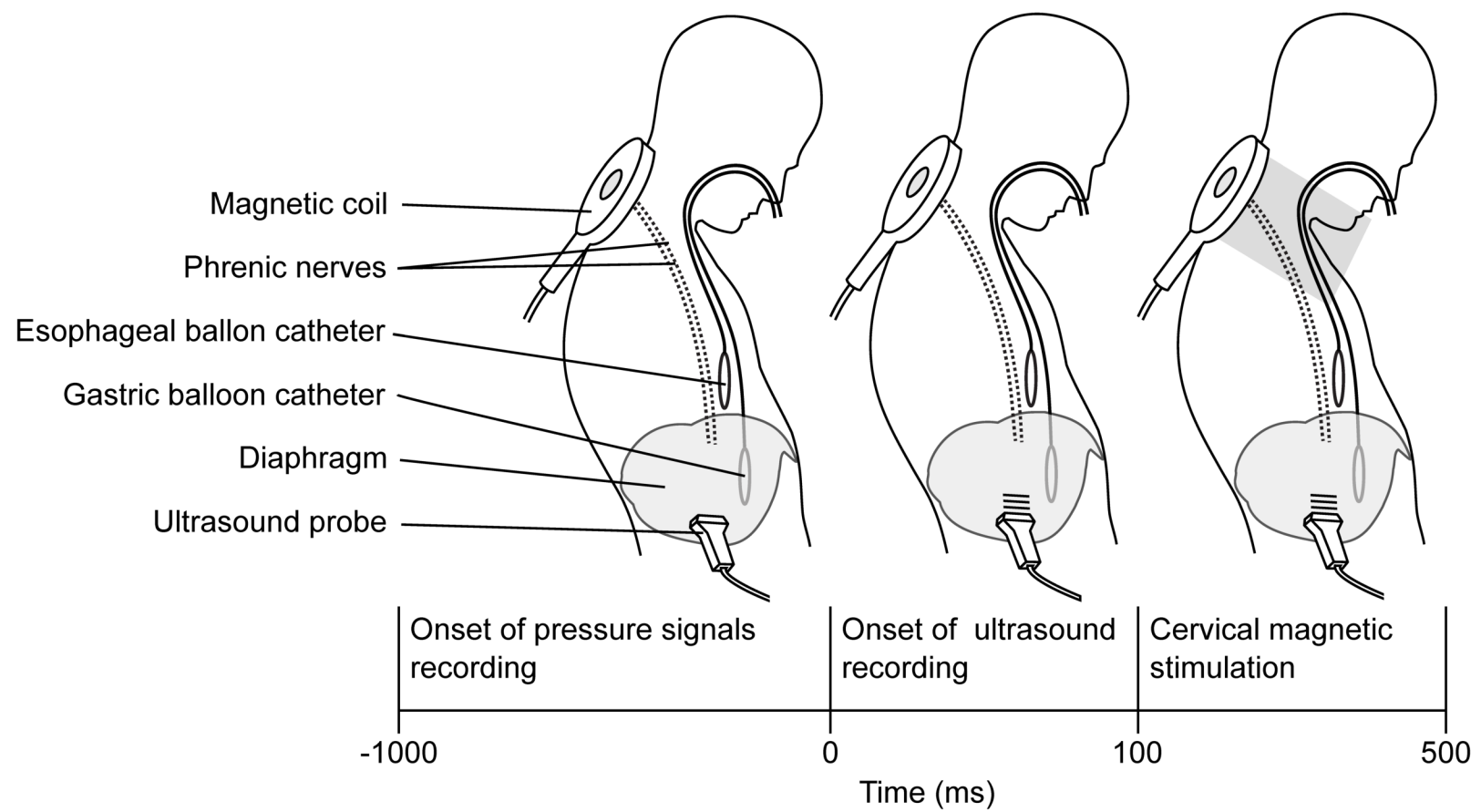
- 611 **Figure 6.** Twitch transdiaphragmatic pressure ($P_{di_{tw}}$, A.), maximal diaphragm tissue velocity
612 ($V_{di_{max}}$, B.), and diaphragm thickening fraction ($TF_{di_{tw}}$, C.) according to stimulation
613 intensities. Box plots present first and third quartiles, in addition to the median. The range
614 over which the data spread out is defined by the whiskers. Repeated measure ANOVAs were
615 used to assess the effect of stimulation intensity on $P_{di_{tw}}$, $V_{di_{max}}$, and $TF_{di_{tw}}$. Tukey's *post-*
616 *hoc* tests were conducted if a significant main effect of intensity was found. *, significant
617 difference with the preceding stimulation intensity (i.e. -10 %); #, significant difference with
618 the second preceding stimulation intensity (i.e. -20 %). Averaged data points for each
619 participant are displayed for $P_{di_{tw}}$ (D.), $V_{di_{max}}$ (E.), and $TF_{di_{tw}}$ (F.). Red points on panels D,
620 E, and F indicate supramaximality for the given parameter.
- 621 **Figure 7.** Averaged data points for each participant regarding the relationships between
622 twitch transdiaphragmatic pressure ($P_{di_{tw}}$) and maximal diaphragm tissue velocity ($V_{di_{max}}$,
623 A.) and between $P_{di_{tw}}$ and diaphragm thickening fraction ($TF_{di_{tw}}$, B.).

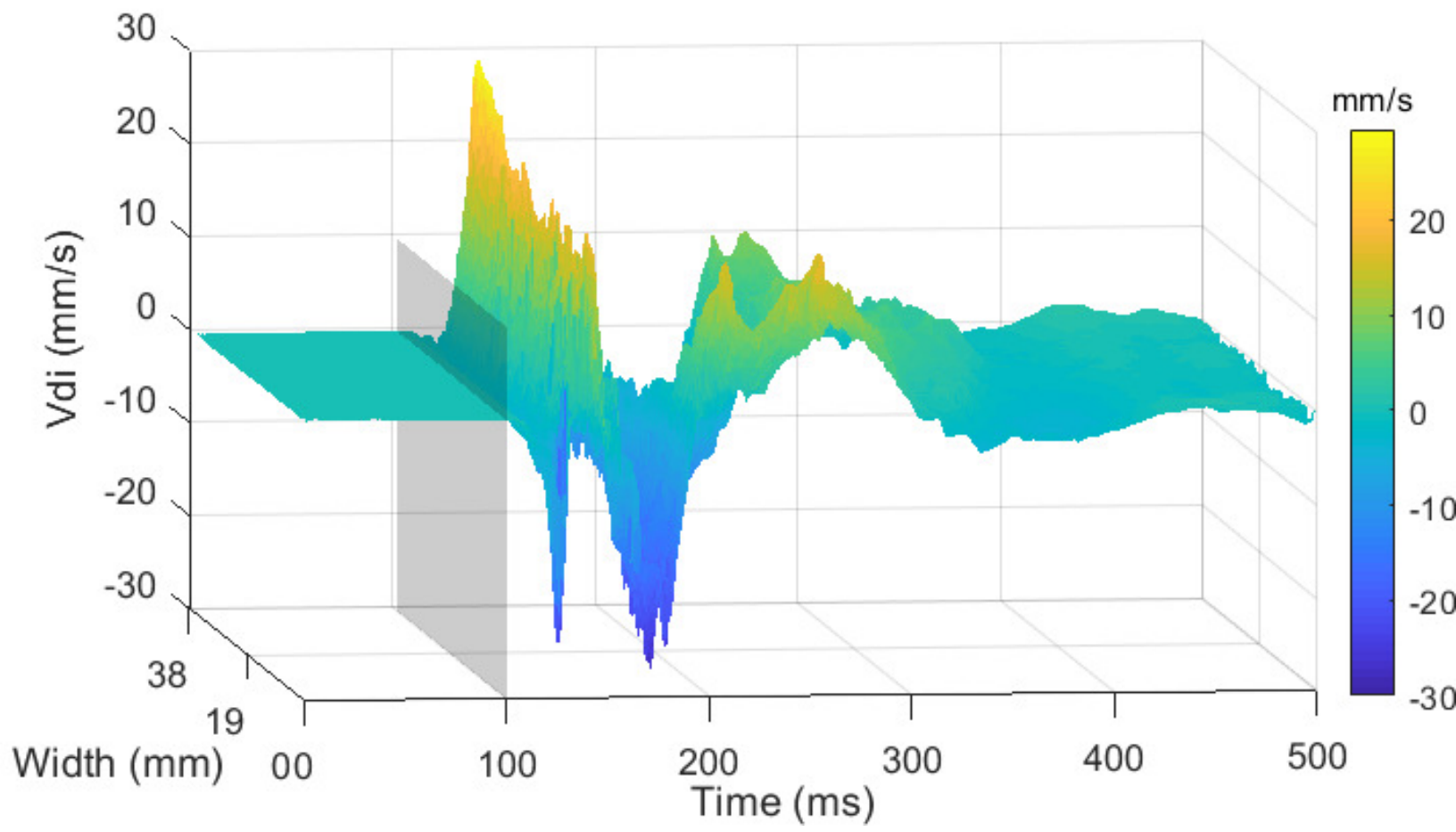
A.



B.



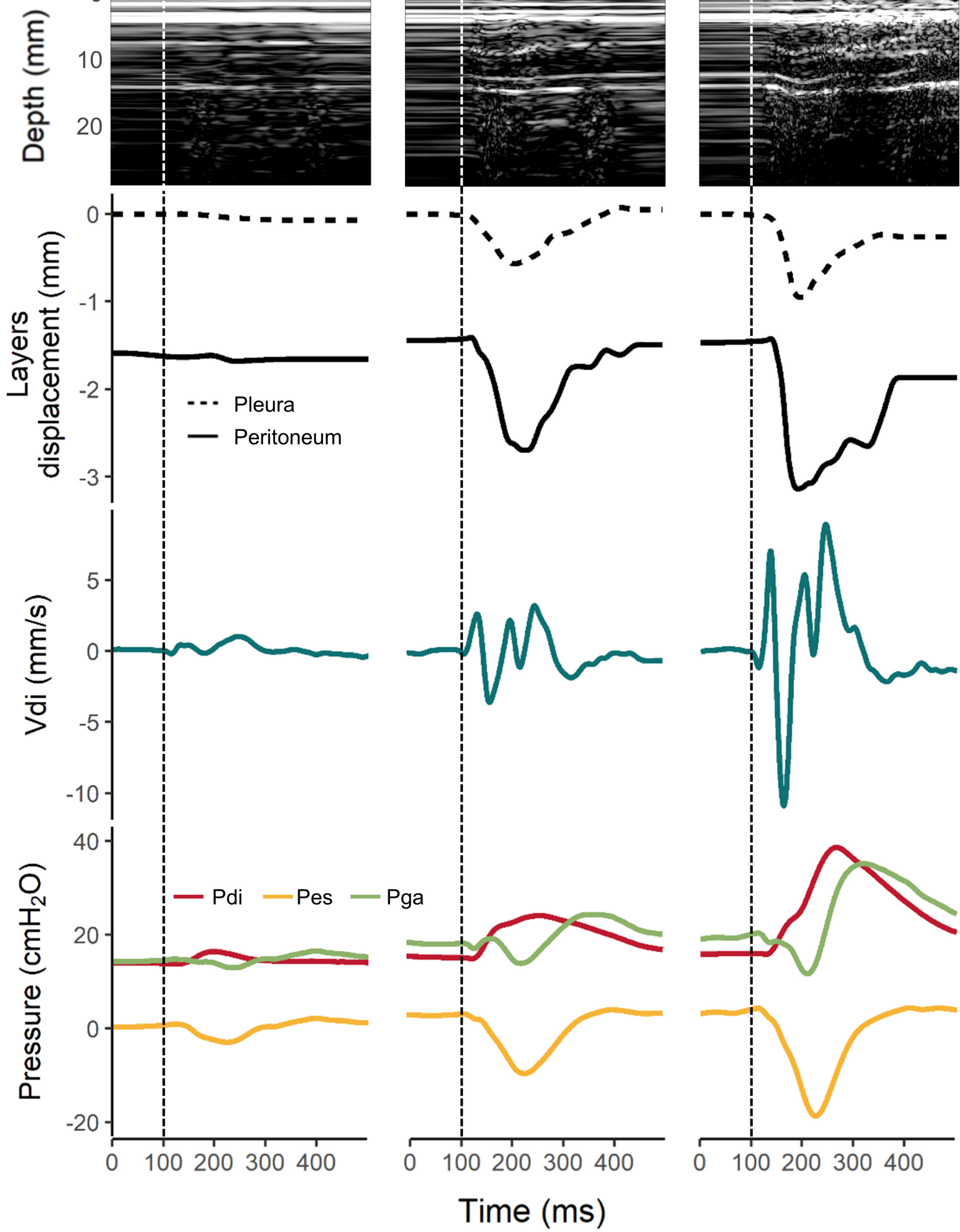


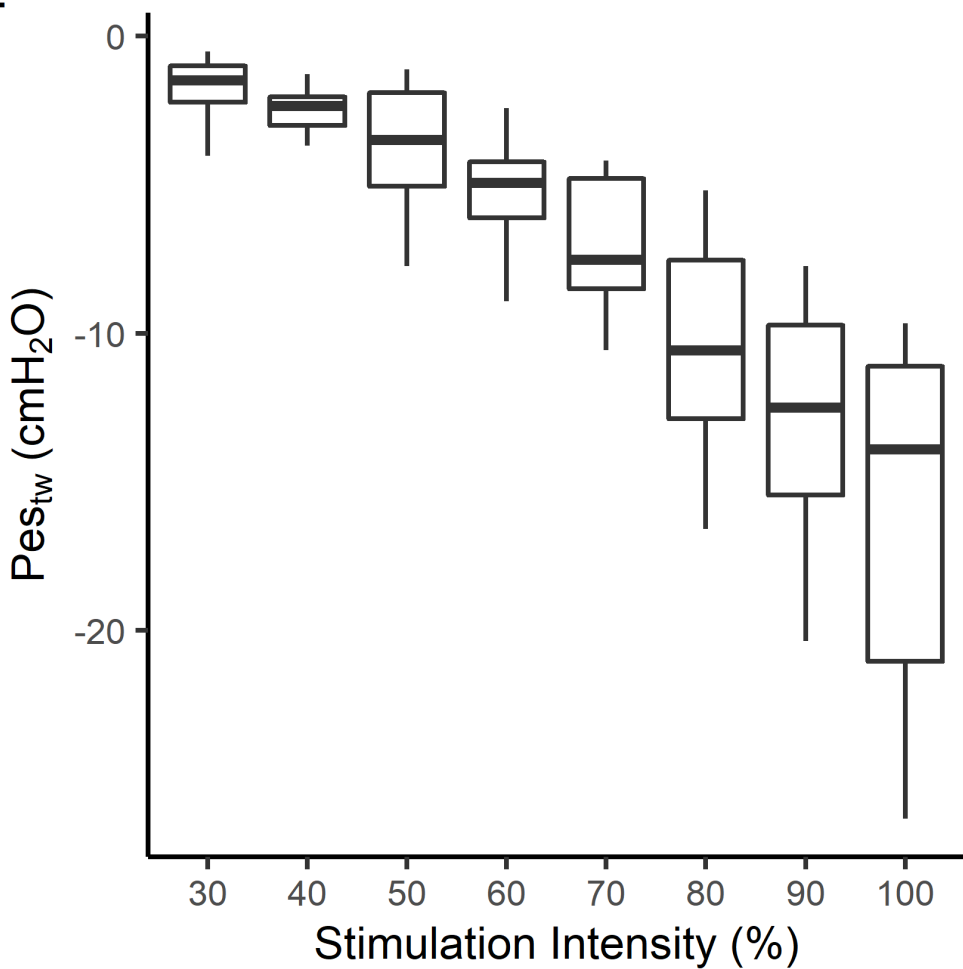
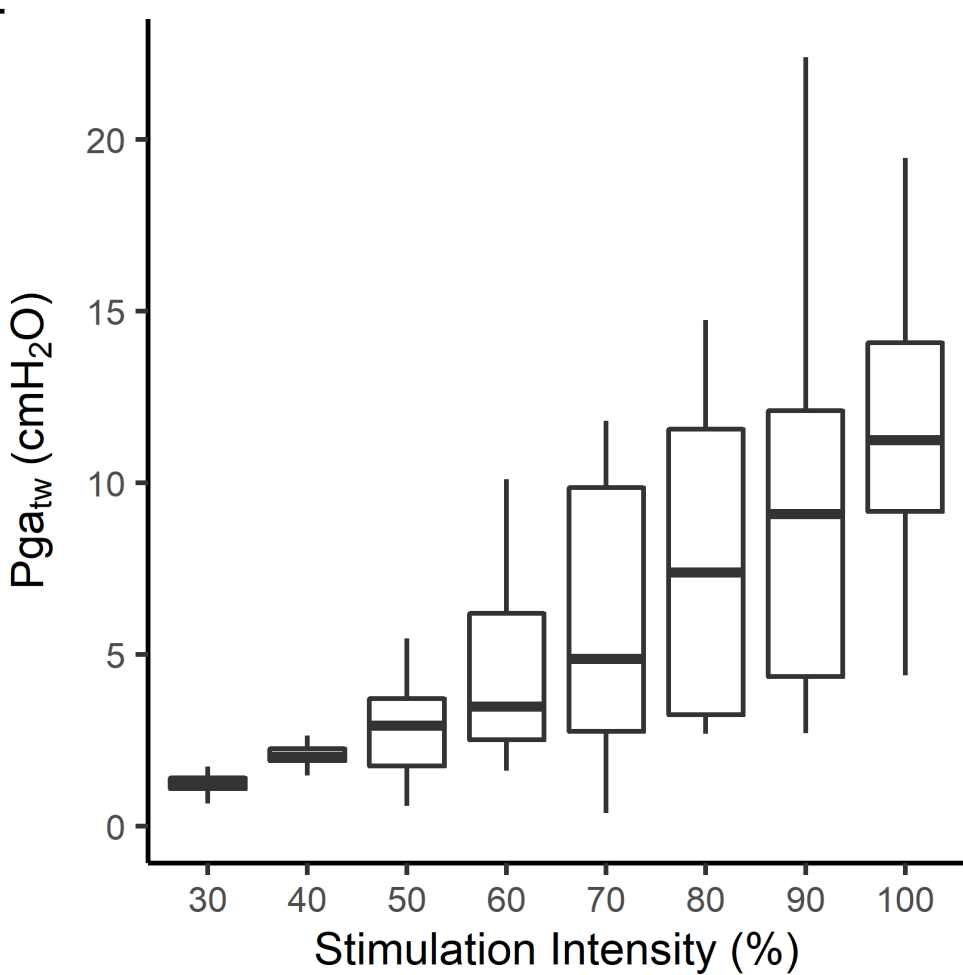


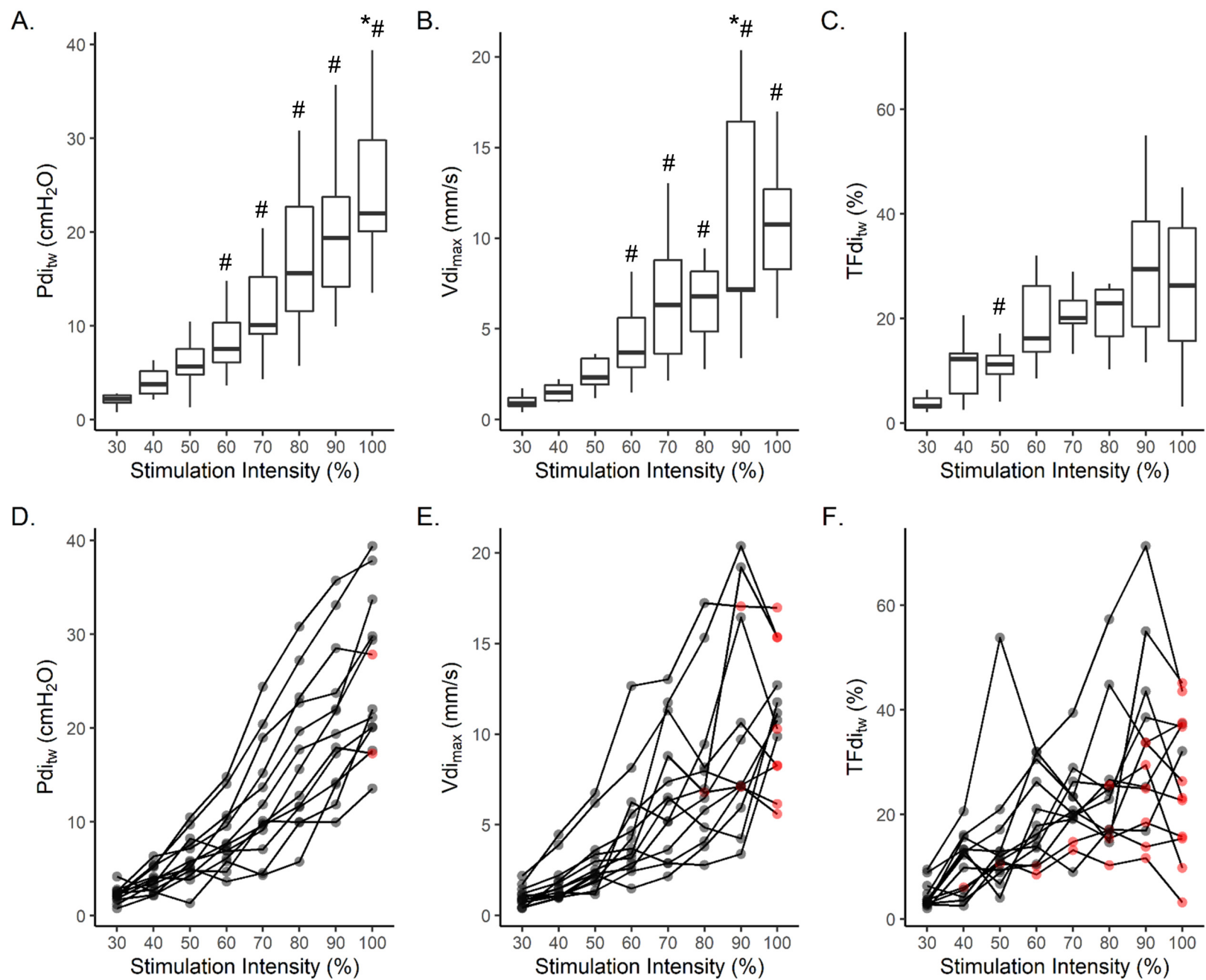
40 %

70 %

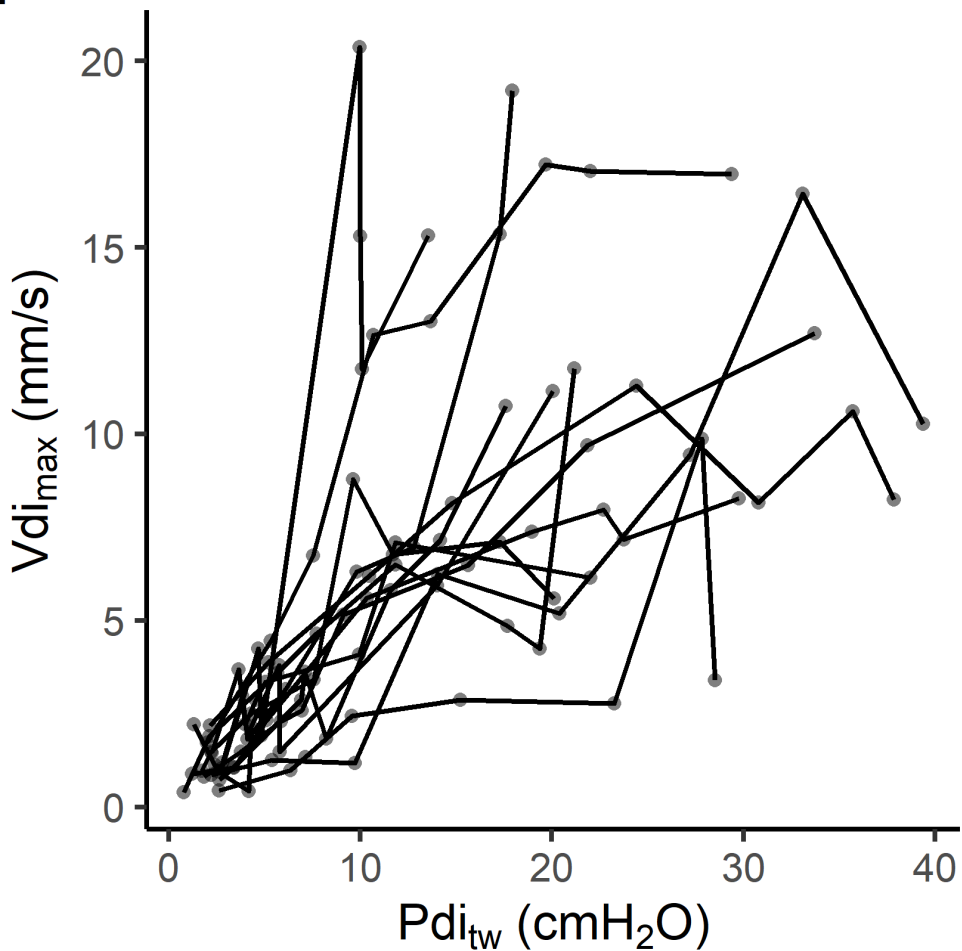
100 %



A.**B.**



A.



B.

